AIAA Journal

VOLUME 29, NUMBER 11

NOVEMBER 1991

FLUID DYNAMICS

Table of Contents continued on back cover

Active Control of Structurally Radiated Noise Using Multiple Piezoelectric Actuators

Bor-Tsuen Wang,* Chris R. Fuller,† and Emilios K. Dimitriadis‡
Virginia Polytechnic Institute and State University, Blacksburg, Virginia 24061

The potential of using multiple piezoelectric actuators to control sound radiated from a harmonically excited rectangular elastic panel is analytically studied. A modal approach in conjunction with quadratic optimal control theory is used to derive the optimal voltages to the piezoelectric actuators necessary to minimize the radiated acoustic power. The results show that an impressive reduction in radiated acoustic power can be achieved with proper choice of size, number, and location of actuators. The performance of multiple independently controlled actuators in attenuating structurally radiated sound is contrasted to that obtained using a single element. It is found that increasing the number of actuators leads to an increase in performance mainly by reducing spillover into unwanted residual modes. The work provides the basis for developing fully distributed actuator systems for active control of sound radiation.

Introduction

In recent years, the problem of actively controlling noise and vibration has generated strong interest in both industry and the engineering research community. Advances in control theory combined with the recent developments in fast computing have made possible the treatment of problems on active structural noise and vibration control that were not feasible only a few years ago. However, it is becoming increasingly clear that the development of corresponding control transducers has generally been lagging behind. Thus, in response to this need, a strong interest has also arisen in new concepts for control actuators and sensors. This paper concerns the use of the recently proposed piezoelectric actuator that consists of layers of piezoelectric material bonded to the surface of the elastic structure to provide control inputs. The problem at hand is that of controlling sound radiation from a baffled rectangular plate, excited by an external noise input.

It has been suggested that a structurally radiated sound can be best suppressed by directly applying active forces to the structure so as to affect the sound radiating vibrations.[1] It was seen in the analysis[1] as well as in the experiments[2] that the point force actuators (i.e., electromagnetic shakers), while providing excellent sound reduction, have some disadvantages, such as their weight/volume and their need for support. Such drawbacks, inherent to point actuators, can be remedied by actuators that are more compact in nature. A type of distributed compact actuator has been developed for the control of beam vibration by Crawley and de Luis.[3] Their actuator consisted of thin strips of piezoelectric material that were bonded to the beam surface and activated to vibrate normal to the polarization direction by oscillating electric voltage.

The basic concept was subsequently extended to develop a two-dimensional actuator bonded to the surface of plates.[4] It was further proposed that the piezoelectric strain can be employed to affect the plate vibrations and to suppress the coupled noise radiation. The feasibility of using a single surface-mounted piezoelectric element to actively control sound transmission through a clamped circular plate was demonstrated.[5] It was shown that when the excitation frequency was low, such that the fundamental mode of vibration was dominant, the radiated field could be significantly attenuated by a single actuator. However, as the frequency of excitation is increased, the modal response and corresponding radiation becomes "richer," and the single actuator appears to be insufficient. Recent preliminary experiments[6] have confirmed these observations and supported the analytical results of Refs. 4 and 5. It is apparent that the appropriate tailoring of the actuators as far as their number, position, and size are concerned becomes increasingly important for higher modes.

It is suggested here that multiple independently controlled piezoelectric actuators should greatly enhance the control effectiveness by further reducing the control spillover. This observation is based on work similar to that of Meirovitch and Norris[7] in which it is demonstrated that as many actuators as modes to be controlled are required. However, in this case, we are only interested in controlling those panel modes that are significant radiators of sound, and this markedly reduces the required number of actuators. In other words, as demonstrated in Ref. 1, the radiated field can be highly attenuated in some cases without significantly reducing panel vibrational amplitude. The present paper is concerned with an analysis of the optimization of the complex voltages needed to be applied to one or more independent piezoelectric actuators so as to minimize the total radiated sound power from a baffled, simply supported, rectangular plate. The noise source for the primary plate excitation is assumed to be a set of one or more noncontacting electromagnetic exciters. The applied force by such a noise source is approximated by a constant amplitude, single frequency, uniformly distributed pressure over a small square area on the plate. This arrangement was chosen so that the results could be compared with future experimental work.

Theoretical Analysis

Plate Vibration

Figure 1 shows the arrangement and coordinates of a baffled, simply supported, rectangular thin plate that is excited by a number of uniformly distributed pressures (noise sources) or by piezoelectric actuators (control sources). To calculate the radiated sound field, a complete description of the plate

Presented as Paper 90-1172 at the AIAA/ASME/ASCE/AHS 31st Structures, Structural Dynamics, and Materials Conference, Long Beach, CA, April 2–4, 1990; received June 29, 1990; revision received Jan. 15, 1991; accepted for publication Jan. 18, 1991.

*Graduate Student, Department of Mechanical Engineering. Student Member AIAA.

†Professor, Department of Mechanical Engineering. Associate Fellow AIAA.

‡Assistant Professor, Department of Mechanical Engineering. Member AIAA.

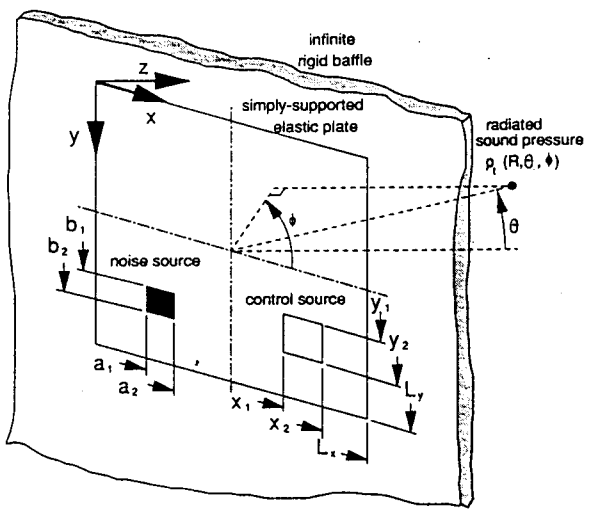

Fig. 1 Arrangement and coordinates of system.

vibration displacement is needed. For the simply supported thin plate, the displacement distribution can be written as

$$w(x,y) = \sum_{m=1}^{\infty}\sum_{n=1}^{\infty} W_{mn} \sin\alpha_m x \sin\beta_n y \tag{1}$$

where

$$\alpha_m = \frac{m\pi}{L_x}$$

$$\beta_n = \frac{n\pi}{L_y}$$

$$W_{mn} = \frac{P_{mn}}{\rho_p h(\omega_{mn}^2 - \omega^2)}$$

Here, $\omega = 2\pi f$ is the excitation frequency, ω_{mn} the plate natural frequency, ρ_p the plate density, h the plate thickness, and P_{mn} the modal force that depends on the exact description of the applied external load. For the present analysis, the plate response is calculated for light fluid loading, and thus radiation loading effects are ignored.

For a uniformly distributed pressure with amplitude q located between coordinates a_1, a_2, b_1, and b_2 as shown in Fig. 1, the modal force can be derived as

$$P_{mn}^n = \frac{4q}{mn\pi^2}(\cos\alpha_m a_1 - \cos\alpha_m a_2)(\cos\beta_n b_1 - \cos\beta_n b_2) \tag{2}$$

where the superscript n will hereafter signify the noise source. The corresponding expression of the modal force for piezoelectric excitation P_{mn}^c has been derived in Ref. 4 as

$$P_{mn}^c = \frac{4C_0\varepsilon_{pe}}{mn\pi^2}(\alpha_m^2 + \beta_n^2)(\cos\alpha_m x_1 - \cos\alpha_m x_2)(\cos\beta_n y_1 - \cos\beta_n y_2) \tag{3}$$

where x_1, x_2, y_1, and y_2 are the coordinates of the piezoelectric actuator. The parameter $C_0\varepsilon_{pe}$ was defined in Ref. 4 for an actuator consisting of two identical piezoceramic patches bonded symmetrically on the two opposite surfaces of plates and driven 180 deg out of phase. The C_0 is a constant that is a function of material properties and dimensions; $\varepsilon_{pe} = d_{31}V/t$ is the strain induced in an unconstrained piezoelectric layer of thickness t when a voltage V is applied along its polarization direction, and d_{31} is the piezoelectric strain constant, a material property.

Sound Radiation

The sound radiation caused by the vibration from either type of source is related to the plate acceleration distribution. Junger and Feit[8] used the stationary phase method on Rayleigh's integral to derive a general expression for the sound pressure. Here, the derivation in Ref. 8 was made specific for the vibration distributions resulting from the noise source as well as from the piezoelectric excitation. Thus, for N_s noise sources and N_c piezoelectric actuators, the sound pressure radiated to a point $p(R, \theta, \phi)$ in the far field was derived (by superposition) for noise sources:

$$p_n(R,\theta,\phi) = K\sum_{i=1}^{N_s}\sum_{m=1}^{\infty}\sum_{n=1}^{\infty} W_{mni}^n I_m I_n \tag{4}$$

and for piezoelectric excitation:

$$p_c(R,\theta,\phi) = K\sum_{i=1}^{N_c}\sum_{m=1}^{\infty}\sum_{n=1}^{\infty} W_{mni}^c I_m I_n \tag{5}$$

where the constant K and the quantities I_m and I_n can be found in Roussos[9] as functions of (ω, θ, ϕ).

When noise sources and piezoelectric actuators act simultaneously for steady-state harmonic excitation, the resulting sound pressure field can be viewed as a superposition of the above given sound pressure. The total pressure can be conveniently written as

$$p_t = p_n + p_c = \sum_{i=1}^{N_s} q_i B_i + \sum_{j=1}^{N_c} (C_0\varepsilon_{pe})_j A_j \tag{6}$$

where B_i and A_j are the sound pressure distribution functions for noise sources and piezoelectric actuators, respectively, given by

$$B_i = K\sum_{m=1}^{\infty}\sum_{n=1}^{\infty} Q_{mni}^n I_m I_n \tag{7}$$

and

$$A_j = K\sum_{m=1}^{\infty}\sum_{n=1}^{\infty} Q_{mnj}^c I_m I_n \tag{8}$$

where

$$Q_{mni}^n = \frac{W_{mni}^n}{q_i} \tag{9}$$

and

$$Q_{mnj}^c = \frac{W_{mnj}^c}{(C_0\varepsilon_{pe})_j} \tag{10}$$

Optimal Control

The control of the radiated noise fields can be achieved by appropriately choosing the piezoelectric voltage parameter $C_0\varepsilon_{pe}$. To provide maximum global reduction in sound pressure, it is customary to minimize the total sound power radiated into the far field. The cost function chosen to be minimized here is the integral of the mean squared sound pressure over a hemisphere of radius R in the far field.[1] This cost function can be written as

$$\Phi = \frac{1}{R^2}\int_s |p_t|^2\, ds = \int_0^{2\pi}\int_0^{\pi/2} |p_t|^2 \sin\theta\, d\theta\, d\phi \tag{11}$$

and it is proportional to the radiated sound power. It should be stressed here that although the control action is applied

directly to the structure, the cost function is derived from the radiated pressure. This characteristic should be contrasted to more obvious approaches in which the plate vibration is minimized. Naturally, attenuating plate vibration will lead to a reduction in sound radiation. However, previous work[1] has demonstrated that this latter approach is an "overkill," and much more subtle and efficient control can be enacted when the far-field radiated pressure is used as an error variable.

When the expression for p_t from Eq. (6) is substituted into Eq. (11), it becomes clear that the cost function is quadratic in the vector of the complex voltage parameters. Therefore, the cost function will possess a unique minimum. A minimization procedure for a quadratic function developed by Lester and Fuller[10] using tensor calculus is based upon the concept of setting the gradient of the cost function with respect to the optimized vector $\bar{p}$ to zero and was applied for the following derivations.

The total pressure can be expressed in vector form:

$$p_t = \bar{B}^T \bar{q} + \bar{A}^T \bar{p} \tag{12}$$

where

$$\bar{B} = \begin{bmatrix} B_1 \\ B_2 \\ \cdot \\ \cdot \\ \cdot \\ B_{N_s} \end{bmatrix}_{N_s \times 1} \tag{13}$$

$$\bar{A} = \begin{bmatrix} A_1 \\ A_2 \\ \cdot \\ \cdot \\ \cdot \\ A_{N_c} \end{bmatrix}_{N_c \times 1} \tag{14}$$

$$\bar{q} = \begin{bmatrix} q_1 \\ q_2 \\ \cdot \\ \cdot \\ \cdot \\ q_{N_s} \end{bmatrix}_{N_s \times 1} \tag{15}$$

$$\bar{p} = \begin{bmatrix} (C_0\varepsilon_{pe})_1 \\ (C_0\varepsilon_{pe})_2 \\ \cdot \\ \cdot \\ \cdot \\ (C_0\varepsilon_{pe})_{N_c} \end{bmatrix}_{N_c \times 1} \tag{16}$$

Then

$$|p_t|^2 = \bar{p}^T[\overline{AA}^{*T}]\bar{p}^* + 2\text{Real}\{\bar{q}^T[\overline{BA}^{*T}]\bar{p}^*\} + \bar{q}^T[\overline{BB}^{*T}]\bar{q}^* \tag{17}$$

where * denotes complex conjugate and T denotes transpose of matrix. Hence the cost function can be written in matrix form as

$$\Phi = \bar{p}^T[\tilde{A}]\bar{p}^* + 2\text{Real}\{\bar{q}^T[\tilde{BA}]\bar{p}^*\} + \bar{q}^T[\tilde{B}]\bar{q}^* \tag{18}$$

where

$$[\tilde{A}]_{N_c \times N_c} = \int_0^{2\pi}\int_0^{\pi/2} [\overline{AA}^{*T}] \sin\theta \, d\theta \, d\phi \tag{19}$$

$$[\tilde{BA}]_{N_s \times N_c} = \int_0^{2\pi}\int_0^{\pi/2} [\overline{BA}^{*T}] \sin\theta \, d\theta \, d\phi \tag{20}$$

$$[\tilde{B}]_{N_s \times N_s} = \int_0^{2\pi}\int_0^{\pi/2} [\overline{BB}^{*T}] \sin\theta \, d\theta \, d\phi \tag{21}$$

Since

$$[\overline{AA}^{*T}]_{N_c \times N_c} = \begin{bmatrix} A_1 \\ A_2 \\ \cdot \\ \cdot \\ \cdot \\ A_{N_c} \end{bmatrix}_{N_c \times 1} [A_1^* \; A_2^* \; \cdots \; A_{N_c}^*]_{1 \times N_c}$$

$$= \begin{bmatrix} A_1A_1^* & A_1A_2^* & \cdots & A_1A_{N_c}^* \\ A_2A_1^* & A_2A_2^* & & A_2A_{N_c}^* \\ \cdot & \cdot & \cdots & \cdot \\ \cdot & \cdot & & \cdot \\ \cdot & \cdot & & \cdot \\ A_{N_c}A_1^* & A_{N_c}A_2^* & & A_{N_c}A_{N_c}^* \end{bmatrix}_{N_c \times N_c} \tag{22}$$

a typical element of $[\overline{AA}^{*T}]$ is

$$A_rAA_s^* = K_rK_s^* \sum_{k=1}^{\infty}\sum_{l=1}^{\infty}\sum_{m=1}^{\infty}\sum_{n=1}^{\infty} Q_{klr}^c \, Q_{mns}^{c*} \, I_{klr}^c \, I_{mns}^{c*} \tag{23}$$

and then for a typical element of $[\tilde{A}]_{N_c \times N_c}$

$$\tilde{A}_{rs} = \int_0^{2\pi}\int_0^{\pi/2} K_rK_s^* \sum_{k=1}^{\infty}\sum_{l=1}^{\infty}\sum_{m=1}^{\infty}\sum_{n=1}^{\infty} Q_{klr}^c \, Q_{mns}^{c*} \, I_{klr}^c \, I_{mns}^{c*} \sin\theta \, d\theta \, d\phi \tag{24}$$

Similarly, a typical element of $[\tilde{BA}]_{N_s \times N_c}$ is as follows:

$$\tilde{BA}_{rs} = \int_0^{2\pi}\int_0^{\pi/2} K_rK_s^* \sum_{k=1}^{\infty}\sum_{l=1}^{\infty}\sum_{m=1}^{\infty}\sum_{n=1}^{\infty} Q_{klr}^n \, Q_{mns}^{c*} \, I_{klr}^n \, I_{mns}^{c*} \sin\theta \, d\theta \, d\phi \tag{25}$$

and a typical element of $[\tilde{B}]_{N_s \times N_s}$

$$\tilde{B}_{rs} = \int_0^{2\pi}\int_0^{\pi/2} K_rK_s^* \sum_{k=1}^{\infty}\sum_{l=1}^{\infty}\sum_{m=1}^{\infty}\sum_{n=1}^{\infty} Q_{klr}^n \, Q_{mns}^{n*} \, I_{klr}^n \, I_{mns}^{n*} \sin\theta \, d\theta \, d\phi \tag{26}$$

Since $(\bar{q}^T[\tilde{B}]\bar{q}^*)$ is a constant, the pay-off function $\tilde{\Phi}$ can then be redefined as

$$\tilde{\Phi} = \Phi - \bar{q}^T[\tilde{B}]\bar{q}^* \tag{27}$$

If we let

$$\bar{F}^T = -\bar{q}^T[\tilde{BA}] \tag{28}$$

then the optimal solution for the pay-off function can be found as in Refs. 1 and 10.

$$\bar{p} = [\tilde{A}]^{-1}\bar{F} \tag{29}$$

It is noted that $\bar{p}$ is the optimized vector that is defined in Eq. (16).

Results

A few representative examples are given below to show the effects of number, size, and location of actuators under different noise conditions. All cases considered are below co-

Table 1 Plate specification

$E = 207 \times 10^9$ N/m^2	$\mu = 0.292$	$L_x = 0.38$ m
$\rho_p = 7870$ kg/m^3	$h = 1.5875$ mm	$L_y = 0.30$ m

Table 2 Natural frequencies of plate, Hz

m \ n	1	2	3	4	5
1	69.6	198.3	412.8	713.0	1099.0
2	149.8	278.5	492.9	793.2	1179.2
3	283.5	412.1	626.6	926.8	1312.8
4	470.6	599.3	813.7	1113.9	1499.9
5	711.1	839.9	1054.3	1354.5	1740.5

incidence. Table 1 shows the specifications of the steel plate used in the simulations. Natural frequencies are tabulated in Table 2.[11] Notice, for the following results, that no damping was included in the analysis. To calculate the plate response and radiated field, it was necessary to truncate the modal sums in the above equations. Upon consideration of computing time, k, l, m, and n were truncated at 5 (i.e., 25 modes considered), and it was found to provide sufficient convergence of this series of Eq. (1). This effectively limits the input noise frequency such that $f \ll 1740$ Hz. Likewise it was necessary to numerically evaluate the above integrals, and this was carried out using the Simpson's one-third rule approach.

The following results consist of the distribution of plate vibrational amplitude plotted along the $y = L_y/2$ horizontal plate midline. The results are normalized by the largest amplitude obtained in each case. Radiation directivity patterns are also presented again along the $y = L_y/2$. For convenience, all θ angular positions to the left of the origin in the directivity pattern plots below correspond to $\phi = \pi$ far-field positions. Similarly, the right half of each plot corresponds to $\phi = 0$. In this case, the input noise amplitude is fixed at $q = 2 \times 10^6$N/m^2, which gives an input force of 3200 N, and assuming the plate is radiating into air, the radiated pressure is plotted in decibels relative to 2×10^{-5}Pa. The radiated pressure was calculated at a distance of 1.8 m from the plate central origin. These variables, as well as radiated acoustic power in decibels relative to 10^{-12}W, are presented for a range of frequencies and different noise source arrangements to demonstrate the effectiveness of the multiple piezoelectric induced control.

Effect of Number of Actuators

Figure 2 presents the vibration amplitude distribution of the plate for differing number and arrangement of piezoelectric control actuators, when the noise excitation frequency was 68.4 Hz, near the resonance frequency of the (1,1) mode given in Table 2. At the top of Fig. 2 and all the following figures, the plate with prescribed noise source and actuator locations and size are drawn to scale looking into the plate from the radiated field. The black blocks represent noise sources, while the shaded blocks are piezoelectric actuators.

In Fig. 2, the solid line depicts the displacement distribution for the noise field, and it can be seen to be very close to that

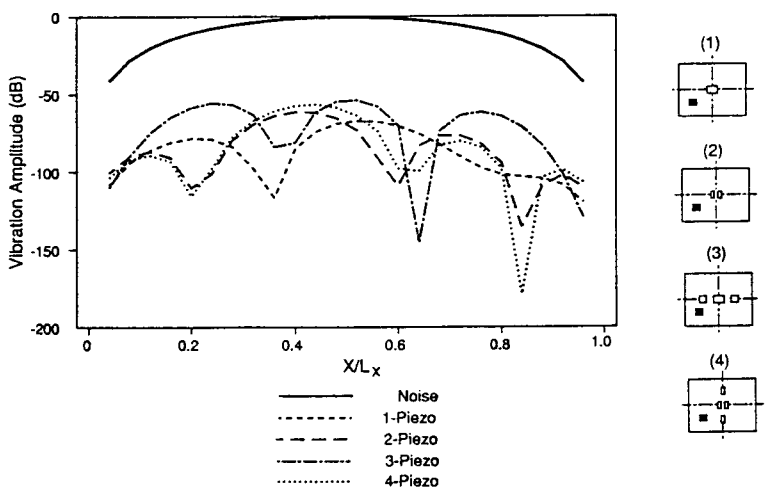

Fig. 2 Vibration amplitude for different number of actuators, f = 68.4 Hz.

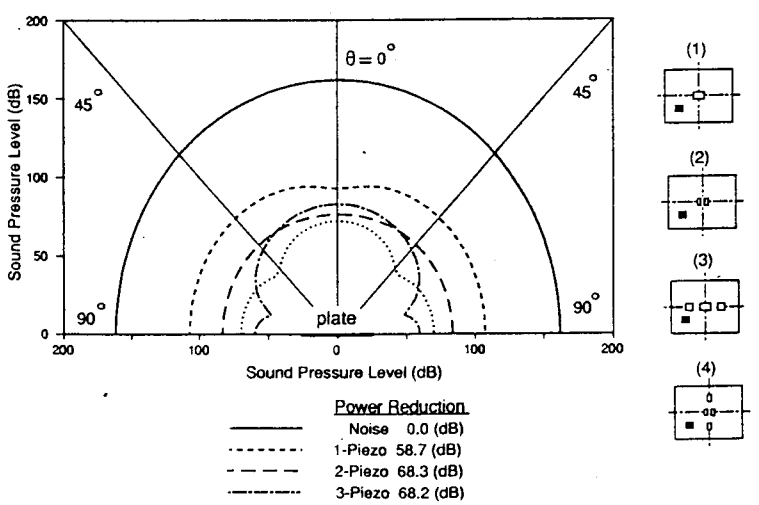

Fig. 3 Radiation directivity for different number of actuators, f = 68.4 Hz.

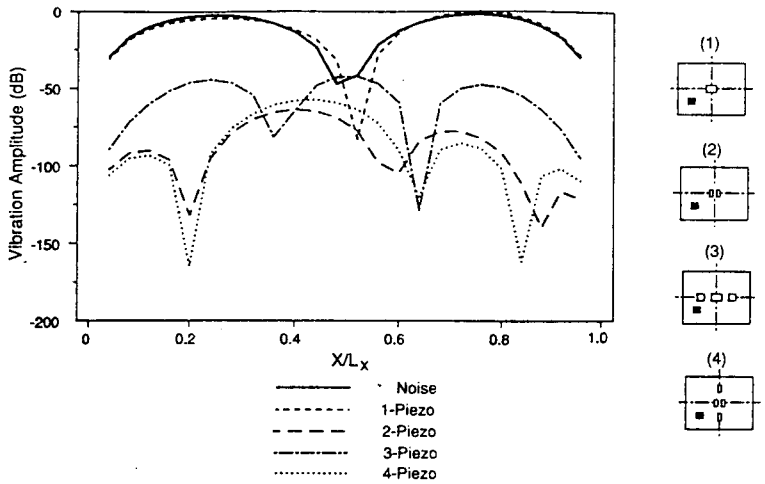

Fig. 4 Vibration amplitude for different number of actuators, f = 148.8 Hz.

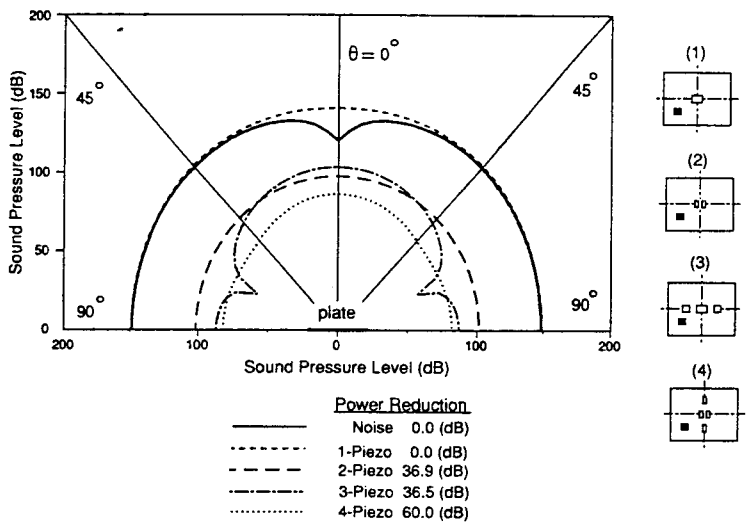

Fig. 5 Radiation directivity for different number of actuators, f = 148.8 Hz.

of the (1,1) mode as expected. When the various configuration of control actuators were applied, the vibration amplitudes were significantly reduced, and the (1,1) mode was well controlled for all cases.

Figure 3 shows the corresponding radiation directivities to the cases of Fig. 2. As expected, the (1,1) mode dominates the radiated noise field due to its high structural response and radiation efficiency. When one actuator was used, the (1,1) mode is controlled, and the (2,1) mode becomes significant. By applying two actuators as shown in Fig. 3, the (1,1) modes and the (2,1) modes can be controlled simultaneously, still leaving the (1,1) mode to contribute significantly to the residual radiation field. Further reduction is observed with the use of three and four actuators, and the residual sound field appears to be composed of a combination of the (3,1) and (1,1) modes. Additionally, the total reduction in radiated acoustic power is shown at the bottom of Fig. 3 in decibels. It is apparent that, for this frequency, as the number of (appropriately positioned) actuators is increased, the corresponding radiated acoustic power decreases.

Next, Figs. 4 and 5 show the vibration amplitude distribution and sound radiation directivity for different actuator configurations and a noise excitation frequency of 148.8 Hz near the (2,1) resonance frequency of Table 2. The results of Fig. 4 indicate that the displacement distribution of the noise is close to the (2,1) mode with some (1,1) contribution (as the driving frequency is not right on resonance). When one actuator located in the center of the plate is used, very little control is achieved, as the actuator in this position cannot couple into the (2,1) mode. In fact, the displacement distribution becomes more symmetric and lobe indicating that the (1,1) mode has been controlled. When two actuators are used as shown in the scale diagrams, the (2,1) mode is significantly reduced, and the (3,1) mode becomes the dominant residual mode. Increasing the number of actuators to three and then four leads to further small reductions in the amplitude. However, the main effect is that the displacement distribution becomes far more complex. This complex distribution in conjunction with phase reversals across the plate leads to a low radiation efficiency and a reduction in radiated power without significantly controlling the plate vibration as shown in Figs. 4 and 5. Similar results have been seen in Refs. 1 and 5. This behavior is apparently due to the actuators controlling the lower-order panel modes and leaving the more complex higher-order modes, which also have lower radiation efficiency, as residuals.

Figure 5 indicates that for a noise input frequency of 148.8 Hz, the (2,1) mode dominates the radiation field. When one actuator is employed, it can be seen from Fig. 5 that virtually no reduction is achieved. It can also be seen that for the $L_y/2$ plane the sound levels near $\theta = 0$ have increased with one control applied. However, out of this plane the levels should have slightly reduced leading to a 0.02 dB reduction in total radiated power. When two actuators are employed, significant reductions are now achieved. Increasing the number of actuators to three has little effect, as the centrally located actuators do not effectively couple into important n modes. However, when four actuators, arranged as shown in

Fig. 5, are used to control the m- and n-modal response simultaneously, a further reduction in radiated levels and corresponding radiated power is achieved.

Figure 6 shows the radiation directivity for the same actuator and noise configurations for a noise excitation frequency of 108 Hz, i.e., an off-resonance excitation case located between the (1,1) and (2,1) modes. For this noise input, the (1,1) mode dominates the radiated noise field, as the (1,1) mode has a high structural response and radiation efficiency. When one actuator was used as shown in Fig. 6, the radiated field is somewhat reduced but not nearly to the degree of the resonance case of Fig. 3. This is also illustrated by the corresponding total power reductions that are 16.9 and 58.7 dB, respectively.

This behavior can be understood with the help of the radiation patterns in Fig. 6. For the case of one actuator, it is apparent that two modes, the (1,1) and (2,1), are contributing to the radiated field, as evidenced by the slight dip at $\theta = 0$ deg. Thus the single actuator minimizes the field by acting on the (1,1) mode whereas the (2,1) mode becomes important. The optimal voltage is then a compromise between the contribution of each mode, i.e., further minimizing the (1,1) mode will lead to an increase in the (2,1) due to spillover and vice versa.

By applying two actuators, Fig. 6 shows that further reduction is possible by controlling the (2,1) and (1,1) simultaneously. Increasing the number of actuators from three and then four leads to increased attenuation, as more modes are simultaneously controlled. The final residual radiation field appears to have contributions from both the (3,1) and (1,1) modes.

The off-resonance case thus requires more actuators for high control due to the number of modes responding relatively strongly being higher. The importance of the (1,1) mode, due to its high radiation efficiency, is evident through the residual plots of Fig. 6.

Finally, Fig. 7 presents the radiated acoustic power over a range of frequencies up to $kL_x = 6.96$. The solid line denotes the radiated acoustic power for the noise source alone. The several peaks occur where natural frequencies are located, and the plate response is high. Note, however (for example), that large peaks are not observed at the (2,1), (1,2), and (2,2) frequencies, since modes have a low radiation efficiency there.

It is clear from Fig. 7 that when the piezoelectric actuators are located along the $L_y/2$ axis, the effective noise control at low frequencies, including the (1,1), (2,1), and (3,1) modes, is obtained. However, for this symmetric configuration, the (1,2), (2,2), and (1,3) modes are uncontrollable, as can be observed, but increasing the piezoelectric actuators to four (case 4 with some positioned off the $y = L_y/2$) leads, nevertheless, to improved broadband power reduction. At very high frequencies, $f \simeq 1000$ Hz, very little attenuation is obtained due to the high modal density of the plate response and the increase in plate radiation efficiency for high kL_x.

The results of Fig. 7 are very encouraging because they predict that the radiated power from the plate can be controlled over the frequency range from $0 < f \leq 750$ Hz with just four actuators. Table 2 shows that the number of plate

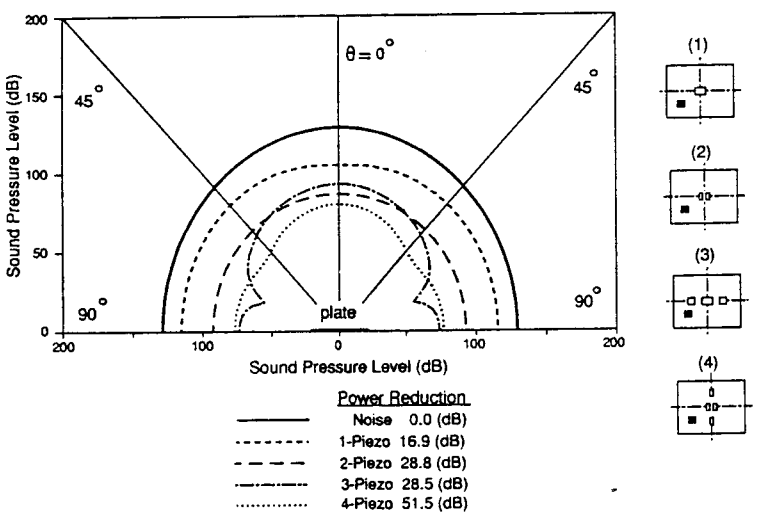

Fig. 6 Radiation directivity for different number of actuators, $f = 108.0$ Hz.

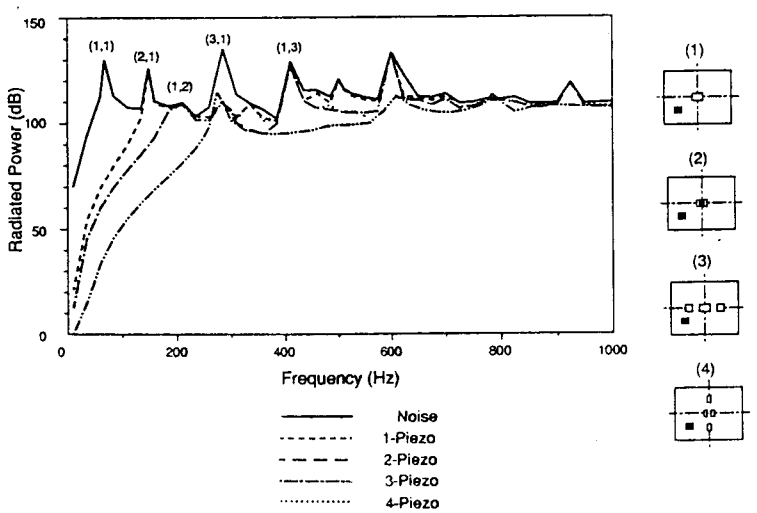

Fig. 7 Radiated power for different number of actuators.

Table 3 Effect of size of actuators, f = 68.4 Hz

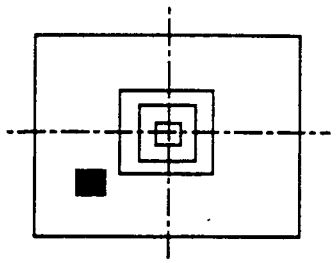

Case	Size of piezoceramic patch $x \times y$, cm × cm	Voltage of piezoceramic patch, V	Radiated power reduction, dB
1	1 × 1	221.55	
2	2 × 2	55.51	
3	3 × 3	24.76	
4	4 × 4	14.00	
5	6 × 6	6.32	
6	10 × 10	2.38	58.7
7	12 × 12	1.71	
8	15 × 15	1.16	
9	20 × 20	0.75	
10	38 × 30	0.47	

Table 4 Effect of size of actuators, f = 148.8 Hz

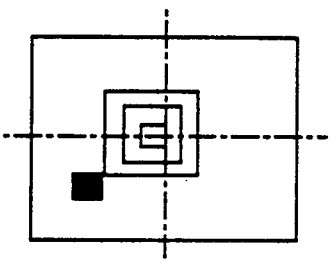

Case	Size of piezoceramic patch $x \times y$, cm × cm	Voltage of piezoceramic patch, V	Radiated power reduction, dB
1	2 × 2	119.00	15.1
2	4 × 4	30.31	15.1
3	6 × 6	13.90	15.0
4	8 × 8	8.17	14.9
5	10 × 10	5.54	14.8
6	14 × 14	3.31	14.5

modes encompassed in this frequency range is 13. This result illustrates the efficiency of the control approach.

Effect of Size of Actuators

To study the size effects of the actuators, a single noise source and single actuator with a fixed central (of the actuator) location was studied for two frequencies. For Table 3, the center of the patch is at x = 190 mm, y = 150 mm. For Table 4, the center of the patch is located at x = 170 mm, y = 150 mm, in other words, asymmetrically positioned so that it can couple into the (2,1) mode. Tables 3 and 4 give the required optimal control voltage amplitude (for q = 1 N/m^2) for a driving frequency of 68.4 and 148.8 Hz, respectively. Again, on the top of the tables, the location of the noise input and actuator is symbolically shown.

Table 3 demonstrates that when the size of the actuator was increased, although the power reduction was generally the same, the optimal voltage was decreased. Similar results can be observed in Table 4. It may be concluded that (at least for the two cases considered here) the size of the piezoceramic patch does not appear to significantly affect noise reduction. However, the input voltages of the actuators are strongly dependent upon size. Thus it is essential to choose the proper size of actuators such that the applied voltages are in the specified operating range for the piezoelectric material. Of course, for other driving frequencies when the expanding patch may cross nodal lines of important modes, then different results may be obtained. The above examples are meant only to illustrate an important operating characteristic of the piezoelectric element.

Effect of Location of Actuators

Figures 8 and 9 show the vibration amplitude distribution and radiation directivity for noise sources arranged to excite the (2,1) mode at 148.8 Hz near the (2,1) mode resonance frequency. When one actuator located in the center of the plate is used, no control is achieved because the actuator cannot couple into the (2,1) mode. Next, the actuator was moved slightly to the left as shown by case 1b in Fig. 8, so that its edge is located next to the nodal line. In this case, the vibration amplitude is significantly reduced, but the radiation field of Fig. 9 shows only a relatively small reduction in level (although total power is reduced by over 18 dB) due to spillover into the (1,1) mode as can be observed from the uniform radiation pattern. To effectively eliminate the (2,1) mode with little spillover into the (1,1) mode, two independent actuators are needed, as shown for case 2 in Fig. 8. In this case, the vibration amplitude is reduced to be a higher mode order residual, and the radiation field of Fig. 9 shows very high reductions in levels and power.

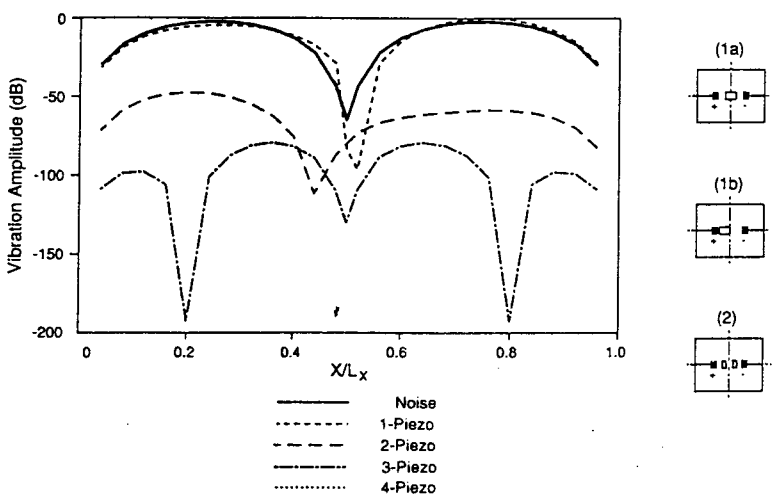

Fig. 8 Vibration amplitude for different location of actuators, f = 148.8 Hz.

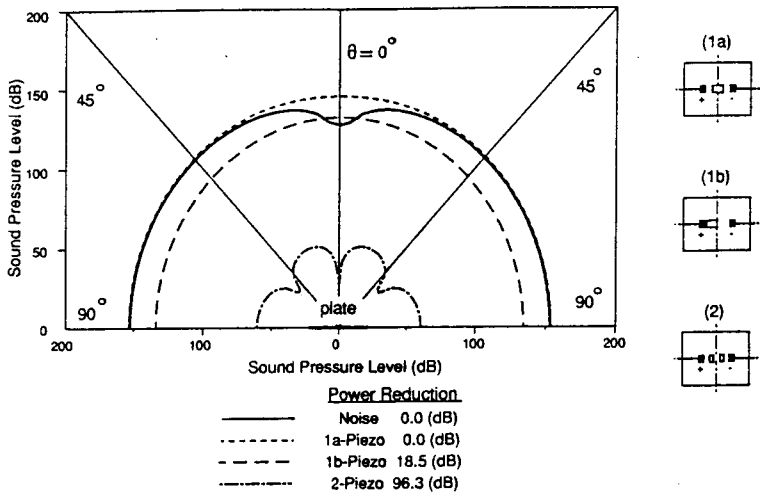

Fig. 9 Radiation directivity for different location of actuators, f = 148.8 Hz.

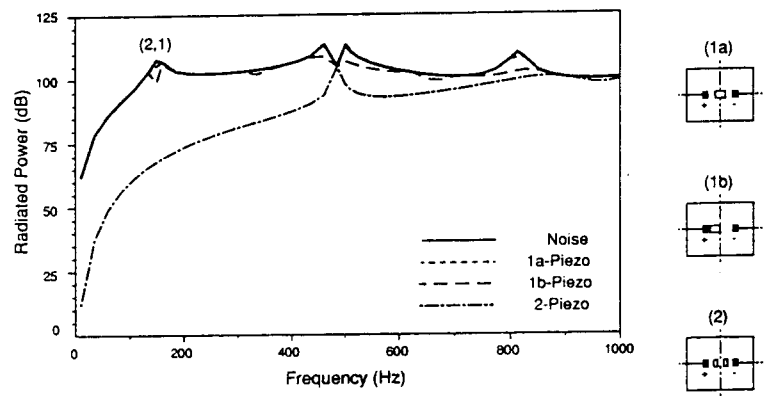

Fig. 10 Radiated power for different location of actuators.

Finally, Fig. 10 shows the radiated acoustic power vs frequency for the configurations of Figs. 8 and 9. The solid line for the noise sources does not demonstrate any high peaks at odd mode natural frequencies due to the arrangement of the noise input. In Fig. 10, the plot is for one centrally located actuator (case 1b) coincident with the noise source; no control is achievable in this position. The actuator next to the (2,1) nodal line (case 1b) can only reduce the radiated power by 18 dB at 148.8 Hz. However, two actuators can be seen to provide high attenuations in radiated acoustic power over a wide range of frequencies.

Conclusions

Active control of structurally radiated sound from a modally responding panel has been analytically studied. The control inputs were multiple independently controllable piezoelectric patches bonded to the panel surface. The work demonstrates that multiple piezoelectric actuators have much potential for control of vibration and its associated radiated noise field. Several significant observations may be summarized as follows:

1) Multiple piezoelectric actuators generally have better noise control characteristics than single actuators due to reduced spillover.

2) The location and number of actuators significantly affect the amount of sound reduction achievable.

3) With proper choice of number and location of actuators, high noise reduction over a broad frequency range up to approximately $kL_x = 5$ for the configurations considered here can be achieved.

4) Within limits, the size of the piezoelectric patch does not appear to significantly effect noise reduction. However, the input optimal voltages are strongly dependent on the size of the piezoceramic patch.

Acknowledgment

The authors acknowledge the support of this work by the Defense Advanced Research Projects Agency and the Office of Naval Research under Grant ONR-N00014-88-K-0721.

References

[1]Fuller, C. R., "Analysis of Active Control of Sound Radiation from Elastic Plates by Force Inputs," *Proceedings of Inter-Noise 88*, 1988, pp. 1061–1064.

[2]Fuller, C. R., Silcox, R. J., Brown, D., and Metcalf, V., "Experiments on Structural Control of Sound Transmitted Through an Elastic Plate," *Proceedings of the American Control Conference*, Pittsburgh, PA, 1989, pp. 2079–2084.

[3]Crawley, E. F., and de Luis, J., "Use of Piezoelectric Actuators as Elements of Intelligent Structures," *AIAA Journal*, Vol. 25, No. 10, 1987, pp. 1373–1385.

[4]Dimitriadis, E. K., Fuller, C. R., and Rogers, C. A., "Piezoelectric Actuators for Distributed Vibration Excitation of Thin Plates," *Journal of Vibration and Acoustics*, Vol. 113, 1991, pp. 100–107.

[5]Dimitriadis, E. K., and Fuller, C. R., "Investigation on Active Control of Sound Transmission Through Elastic Plates using Piezoelectric Actuators," AIAA Paper 89-1062, 1989.

[6]Fuller, C. R., Hansen, C. H., and Snyder, S. D., "Experiments on Active Control of Sound Radiation from a Panel Using a Piezoceramic Actuators," *Journal of Sound and Vibration* (submitted for publication).

[7]Meirovitch, L., and Norris, M. A., "Vibration Control," *Proceedings of Inter-Noise 84*, 1984, pp. 477–482.

[8]Junger, M. C., and Feit, D., *Sound, Structures and Their Interaction*, 2nd ed., MIT Press, Cambridge, MA, 1986, pp. 119–126.

[9]Roussos, L. A., "Noise Transmission Loss of a Rectangular Plate in an Infinite Baffle," NASA TP 2398, March 1985.

[10]Lester, H. C., and Fuller, C. R., "Active Control of Propeller Induced Noise Fields Inside a Flexible Cylinder," AIAA Paper 86-1957, 1986.

[11]Pilkey, W. D., and Chang, P. Y., *Modern Formulas for Statics and Dynamics*, McGraw-Hill, New York, 1978, pp. 330–338.